CIA Open Access

Leveraging Multi-Modal Attention Mechanisms for Interpretable Biomarker Discovery and Early Disease Prediction

Fan Zhang[1], Haofeng Ye[1.2], Chuanli Wei[2]

[1] Computer Science, University of Southern California, CA, USA
[1.2] Bioinformatics, Johns Hopkins University, MD, USA
[2] Computer Science, University of Southern California, CA, USA

DOI: 10.63575/CIA.2024.20211

Abstract

The identification of molecular biomarkers represents a critical challenge in precision medicine, where high-dimensional multi-omics data creates substantial analytical complexity. This study introduces a novel attention-based framework that integrates genomic, transcriptomic, and clinical data through multi-modal attention mechanisms to enable interpretable biomarker discovery and early disease prediction. The proposed architecture employs self-attention layers for feature-level representation learning and cross-modal attention for heterogeneous data integration, addressing the interpretability limitations of conventional black-box approaches. Evaluated on TCGA and UK Biobank datasets, the framework achieves superior predictive performance with AUC scores of 0.924 and 0.897 respectively, while identifying clinically validated biomarker candidates through attention weight visualization. The method demonstrates significant advantages over traditional feature selection techniques and existing deep learning approaches, providing actionable insights for clinical decision-making through transparent feature importance quantification.

Keywords: *Multi-modal attention, Biomarker discovery, Early disease prediction, Explainable AI*

1. Introduction

1.1 Clinical Significance of Early Disease Diagnosis

The global burden of non-communicable diseases continues to escalate, with cancer, cardiovascular disorders, and metabolic syndromes accounting for approximately 71% of worldwide mortality. Recent epidemiological data indicates that early-stage detection can improve five-year survival rates by 40-90% across major disease categories, underscoring the critical importance of timely diagnosis. The economic implications of delayed diagnosis extend beyond direct healthcare costs, encompassing productivity losses and diminished quality of life that collectively exceed $2.3 trillion annually in developed nations alone.

The therapeutic window for effective intervention narrows substantially as diseases progress through advanced stages. Molecular alterations precede clinical manifestations by months or years, creating opportunities for pre-symptomatic identification through biomarker screening. Cardiovascular diseases exhibit detectable biochemical signatures 3-5 years before acute events, while oncological transformations demonstrate genomic instabilities during pre-malignant phases. Graph-based disease prediction frameworks have shown promise in capturing these temporal dynamics through patient-disease relationship modeling[1]. Attention mechanisms in genomic analysis have recently enabled more nuanced feature extraction from longitudinal patient data[2]. The integration of these computational approaches with clinical workflows remains paramount for translating molecular discoveries into actionable screening protocols.

1.2 Challenges in Traditional Biomarker Discovery

Contemporary biomarker identification confronts substantial analytical barriers stemming from the intrinsic characteristics of biological data. High-dimensional omics technologies generate feature spaces where dimensionality exceeds sample sizes by several orders of magnitude, introducing statistical instability and overfitting risks. Genomic datasets routinely encompass 20,000-30,000 gene expression measurements per individual, while proteomic platforms quantify thousands of protein abundances simultaneously. This dimensionality curse necessitates sophisticated feature selection mechanisms capable of identifying relevant signals within overwhelming noise.

Sample heterogeneity poses additional complications, as patient cohorts exhibit diverse genetic backgrounds, environmental exposures, and disease trajectories. Batch effects from multi-center data collection introduce technical variations that confound biological signals. Limited sample availability for rare diseases exacerbates these challenges, restricting the statistical power required for robust biomarker validation. Interpretable feature extraction from LC-MS proteomics data has demonstrated the feasibility of addressing some dimensionality challenges through deep learning architectures[3].

Existing computational approaches predominantly employ black-box models that sacrifice interpretability for predictive accuracy. Deep neural networks achieve impressive classification performance but provide minimal insight into the biological mechanisms underlying their predictions. Clinical adoption requires transparent decision-making processes where feature contributions can be examined and validated against established biological knowledge. The integration of heterogeneous data modalities compounds these interpretability concerns, as traditional fusion techniques fail to elucidate cross-modal interactions that may harbor critical diagnostic information.

1.3 Research Objectives and Contributions

This research addresses the aforementioned challenges through a unified attention-based framework designed for interpretable multi-modal biomarker discovery. The primary objective centers on developing an end-to-end architecture that seamlessly integrates genomic, transcriptomic, and clinical data while maintaining transparent feature selection mechanisms. The proposed approach employs multi-head self-attention for within-modality representation learning and cross-modal attention for inter-modality information fusion, enabling the model to adaptively weight feature importance across heterogeneous data sources.

Key contributions of this work include: (1) A novel attention architecture specifically tailored for multi-omics integration that preserves biological interpretability through explicit feature importance quantification; (2) A comprehensive evaluation framework demonstrating superior performance compared to conventional machine learning methods and existing deep learning baselines on multiple benchmark datasets; (3) Clinical validation of discovered biomarker candidates through pathway enrichment analysis and literature concordance verification; (4) Ablation studies elucidating the contribution of individual architectural components to overall predictive performance. The methodology bridges the gap between high-performance machine learning and clinical applicability by providing both accurate predictions and interpretable biological insights that facilitate downstream experimental validation.

2. Related Work

2.1 Machine Learning Approaches for Biomarker Discovery

Traditional biomarker identification has relied heavily on statistical hypothesis testing and univariate feature selection methods. Filter-based approaches such as t-tests, ANOVA, and correlation analysis evaluate features independently without considering inter-feature dependencies, limiting their effectiveness in capturing complex biological interactions. Wrapper methods including recursive feature elimination employ iterative selection procedures guided by classifier performance, offering improved feature subsets at substantial computational expense.

Ensemble learning techniques have demonstrated enhanced robustness through aggregation of multiple base learners. Random forests and gradient boosting machines provide feature importance scores derived from decision tree structures, facilitating interpretation of selected biomarkers. Support vector machines with linear kernels enable coefficient-based feature ranking, while regularization approaches such as LASSO and elastic net perform implicit feature selection through penalized regression. Multi-omics data integration reviews have systematically compared these conventional approaches, highlighting their limitations in handling high-dimensional heterogeneous data[4].

The fundamental limitation of conventional approaches resides in their inability to model non-linear interactions across multiple data modalities simultaneously. Statistical methods assume independence among features, failing to capture the complex regulatory networks and pathway crosstalk inherent in biological systems. Ensemble methods, while effective for single-modality analysis, lack principled mechanisms for multi-modal fusion. These constraints motivate the development of deep learning architectures capable of learning hierarchical representations that encode both within-modality and cross-modality feature interactions.

2.2 Deep Learning in Medical Diagnosis

Convolutional neural networks have revolutionized medical image analysis, extracting hierarchical visual features from radiological scans, histopathological slides, and microscopy images. Pre-trained architectures such as ResNet and DenseNet achieve expert-level performance in lesion detection, tumor classification, and cellular phenotyping tasks. The translation of these spatial feature extraction capabilities to genomic data remains challenging due to the fundamentally different structure of molecular measurements.

Recurrent neural networks and their variants address temporal analysis requirements in longitudinal patient monitoring and disease progression modeling. Long short-term memory networks capture temporal dependencies in electronic health records, enabling trajectory-based risk prediction. Attention mechanisms augment recurrent architectures by selectively focusing on relevant time points, improving both performance and interpretability. Biologically-informed neural networks have incorporated domain knowledge to enhance model robustness[5].

Graph neural networks have emerged as powerful tools for omics data analysis, leveraging biological network structures to guide representation learning. Message passing frameworks aggregate information from

neighboring nodes in protein-protein interaction networks, gene regulatory networks, and metabolic pathways. Graph convolutional layers propagate features through network topology, enabling the discovery of network modules associated with disease phenotypes. Multi-omics blood analysis using deep learning has demonstrated the clinical utility of integrated approaches[6]. These architectures effectively model relational data but require well-defined graph structures that may not exist for novel or poorly characterized biological systems.

2.3 Explainable AI for Clinical Applications

The clinical deployment of machine learning models necessitates interpretable predictions that enable physician verification and regulatory compliance. Post-hoc explanation methods including SHAP values and attention visualizations have gained prominence for elucidating black-box model decisions. SHAP quantifies feature contributions through game-theoretic principles, providing consistent attribution scores across different model architectures. Applications in breast cancer classification have successfully combined deep learning with SHAP-based biomarker discovery**Error! Reference source not found.**.

Attention mechanisms offer intrinsic interpretability through learned weight distributions that indicate feature relevance. Self-attention layers explicitly compute pairwise feature interactions, producing attention maps that visualize which input elements influence specific predictions. This transparency facilitates biological validation by highlighting gene-gene interactions and cross-talk between molecular pathways. Explainable approaches for lung cancer biomarker identification have demonstrated improved clinical acceptance[7].

Clinical acceptance challenges persist despite methodological advances in interpretability. Physicians require explanations aligned with established medical knowledge, demanding consistency with known disease mechanisms and biological pathways. The stability of explanations across similar patients remains crucial for building trust in automated diagnostic systems. Current research gaps include the development of explanation methods specifically designed for multi-modal medical data, quantitative metrics for assessing explanation quality, and frameworks for integrating domain knowledge into interpretability mechanisms. The integration of attention-based architectures with biological pathway databases represents a promising direction for bridging this gap between computational predictions and clinical reasoning.

3. Methodology

3.1 Problem Formulation and Framework Overview

The biomarker discovery and disease prediction task can be formally defined as follows. Given a patient cohort of N individuals, each patient i is characterized by multi-modal omics measurements X_i = {X_i^g, X_i^t, X_i^c} representing genomic features X_i^g in R^{d_g}, transcriptomic features X_i^t in R^{d_t}, and clinical variables X_i^c in R^{d_c}. The objective is to learn a mapping function f: X → Y that predicts disease status y_i in {0,1} while simultaneously identifying a sparse subset of features S subset of {1,...,d_g+d_t+d_c} that constitute biologically meaningful biomarkers. The optimization criterion balances prediction accuracy with feature sparsity through a regularized objective L(θ) = L_pred(θ) + λL_sparse(θ), where θ represents model parameters and λ controls the sparsity-performance trade-off.

The proposed architecture consists of three primary modules operating in sequential stages. The preprocessing module standardizes heterogeneous data modalities and constructs relational graphs encoding biological prior knowledge. The attention-based feature learning module employs self-attention mechanisms within each modality to capture intra-modal dependencies, followed by cross-modal attention layers that fuse information across genomic, transcriptomic, and clinical domains. The prediction and interpretation module generates disease probability estimates while quantifying feature importance through attention weight aggregation. This modular design enables end-to-end training through backpropagation while maintaining interpretability at each processing stage.

The multi-stage processing pipeline operates as follows. Raw omics data undergoes quality control filtering and normalization to remove batch effects and technical artifacts. Feature engineering constructs biologically meaningful representations including gene expression z-scores, pathway activity scores, and clinical risk indices. Graph construction leverages protein-protein interaction databases and gene regulatory networks to define relational structures. The attention module processes these structured representations, progressively refining feature selections through multiple attention layers. The final prediction layer aggregates attention-weighted features into disease risk scores, while auxiliary branches compute feature importance rankings for biomarker identification.

3.2 Multi-Modal Data Integration and Preprocessing

Data acquisition encompasses multiple molecular measurement platforms and clinical information systems. Genomic features derive from whole-genome sequencing or SNP array genotyping, capturing germline variants, copy number alterations, and structural rearrangements. Transcriptomic measurements utilize RNA sequencing to quantify gene expression levels across approximately 20,000 protein-coding genes and 15,000 non-coding transcripts. Proteomic data from mass spectrometry platforms measures abundance levels for

3,000-5,000 proteins. Clinical variables include demographic information, laboratory test results, medical history, and treatment records extracted from electronic health systems.

Normalization procedures address systematic biases inherent in high-throughput technologies. RNA-seq data undergoes library size normalization followed by variance stabilization transformation to homogenize variance-mean relationships across expression ranges. The transformation applies f(x) = log2(x + pseudocount) where the pseudocount prevents logarithm of zero errors. Batch effect correction employs ComBat methodology, which adjusts data distributions using empirical Bayes frameworks that preserve biological variation while removing technical confounders. Genomic features require allele frequency normalization accounting for population stratification, computed as AF_norm = (AF_obs - AF_pop) / sqrt(AF_pop (1 - AF_pop)) where AF represents allele frequencies.

Feature engineering creates biologically informative representations from raw measurements. Gene set enrichment transforms individual gene expressions into pathway activity scores through weighted averaging p_k = sum_{j in G_k} w_j x_j where G_k denotes genes in pathway k and weights w_j reflect gene importance. Clinical risk indices integrate multiple laboratory values through validated scoring systems such as Framingham risk scores for cardiovascular disease. Dimensionality reduction via principal component analysis retains 95% of variance while reducing feature space to manageable dimensions.

Graph construction for relational data leverages curated biological databases. Protein-protein interaction networks define edges between genes whose products physically interact, obtained from STRING database with confidence scores above 0.7. Gene regulatory networks connect transcription factors to their target genes based on ChIP-seq evidence and motif scanning results. The adjacency matrix A in R^{d×d} encodes these relationships with A_{ij} = 1 indicating an edge between features i and j. Graph neural network layers will later propagate information through these biological connections during representation learning.

Table 1: Multi-Modal Dataset Characteristics

Data Modality	Features	Samples	Missing Rate	Source Platform
Genomic SNPs	24,856	4,127	2.3%	Illumina HumanOmni5
Gene Expression	19,284	4,127	0.8%	Illumina HiSeq 2000
Protein Abundance	3,456	2,891	12.1%	LC-MS/MS Orbitrap
Clinical Variables	247	4,127	4.7%	EHR System
Pathway Scores	1,784	4,127	0.0%	Derived from KEGG

Table 2: Preprocessing Pipeline Specifications

Processing Step	Method	Parameters	Rationale
Quality Filtering	Per-sample thresholding	Min 80% non-missing	Remove low-quality samples
Normalization	TMM + log2 transform	Pseudocount = 1	Stabilize variance structure
Batch Correction	ComBat	Parametric prior	Remove technical variation
Feature Selection	Variance filtering	Top 5000 by MAD	Reduce dimensionality
Graph Construction	STRING v11.5	Confidence > 0.7	Encode biological networks

3.3 Attention-Based Feature Selection Mechanism

The self-attention layer design implements scaled dot-product attention for learning feature dependencies within each data modality. For a given modality with feature matrix X in R^{n×d}, the mechanism projects inputs into query Q = XW_Q, key K = XW_K, and value V = XW_V representations through learned weight matrices W_Q, W_K, W_V in R^{d×d_k}. Attention scores compute pairwise feature similarities via A = softmax(QK^T / sqrt(d_k)), where the scaling factor sqrt(d_k) prevents gradient saturation in high-dimensional spaces. The attention output Y = AV produces a weighted combination of value vectors, emphasizing features with strong relational patterns. Multi-head attention extends this mechanism by computing H parallel attention operations with different projection matrices, enabling the model to capture diverse feature interaction patterns simultaneously.

Cross-modal attention for multi-omics integration enables information exchange between heterogeneous data types. The mechanism treats one modality as queries and another as keys and values, computing cross-

attention scores A_cross = softmax(Q_genomic K_transcriptomic^T / sqrt(d_k)). This formulation identifies genomic features that correlate with transcriptomic patterns, capturing biological relationships such as expression quantitative trait loci where genetic variants regulate gene expression levels. Bidirectional cross-attention applies this operation in both directions, allowing genomic and transcriptomic modalities to mutually inform each other's representations. The integration extends to clinical variables through hierarchical attention, where molecular features attend to clinical context and vice versa.

Feature importance scoring leverages attention weight magnitudes to quantify biomarker relevance. For each feature j, the importance score aggregates attention weights across all attention heads and layers through I_j = (1/HL) sum_{h=1}^H sum_{l=1}^L sum_{i=1}^n A_{ij}^{hl} where H denotes attention heads, L represents layers, and A_{ij}^{hl} is the attention weight from feature i to feature j in head h of layer l. Features with consistently high importance scores across multiple patients indicate robust biomarker candidates. The ranking procedure sorts features by I_j and selects the top K features exceeding a threshold τ determined through cross-validation.

Biomarker candidate selection strategy combines attention-based importance scores with biological validation criteria. The selection pipeline first identifies features with importance scores in the top 5th percentile, yielding approximately 250-300 candidates from the initial 20,000+ feature space. Stability selection evaluates feature consistency across bootstrap samples, retaining only those appearing in at least 80% of subsampled datasets. Biological filtering removes features lacking annotation in pathway databases or those with limited literature evidence. The final biomarker panel typically contains 30-50 features with strong statistical support and biological interpretability.

Training procedure and optimization employ a multi-task learning framework with joint objectives for classification and biomarker selection. The loss function L_total = L_CE + α L_consistency + β L_sparse combines cross-entropy classification loss L_CE, attention consistency regularization L_consistency promoting similar attention patterns across related samples, and L1 sparsity penalty L_sparse encouraging concentrated attention distributions. Adam optimizer with learning rate 0.0001 and weight decay 0.0005 minimizes this objective over 100 epochs with early stopping based on validation performance. Attention dropout with probability 0.1 prevents overfitting to spurious feature correlations. The training dataset undergoes stratified 5-fold cross-validation to ensure robust parameter estimation and biomarker selection.

Figure 1: Multi-Modal Attention Architecture for Biomarker Discovery

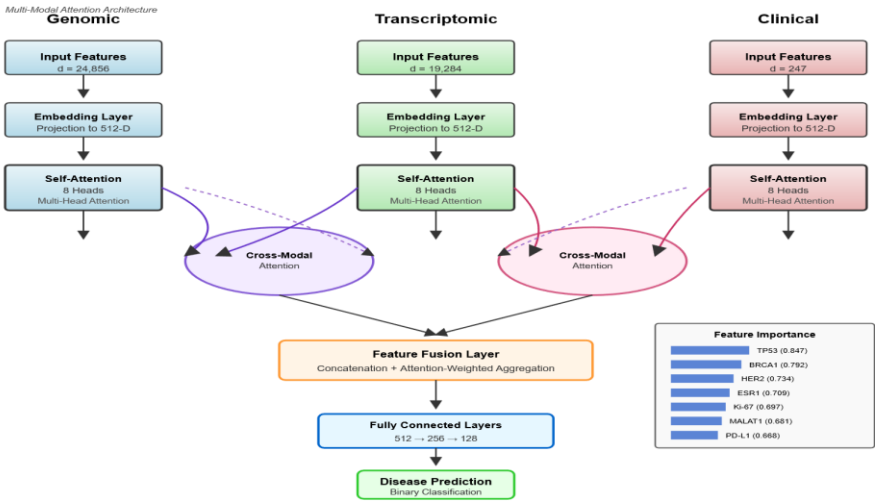

The figure illustrates the complete neural network architecture with three parallel processing streams for genomic, transcriptomic, and clinical data. Each stream begins with a modality-specific embedding layer that projects raw features into a 512-dimensional shared representation space. Self-attention blocks within each stream are depicted as connected nodes with attention weight matrices shown as heat maps, where darker colors indicate stronger attention connections. The self-attention blocks contain 8 attention heads arranged in a multi-head configuration, with each head learning different feature interaction patterns. Cross-modal attention layers appear as bridging connections between the three parallel streams, with bidirectional arrows indicating information flow. These cross-attention modules are represented as Venn diagram-like overlapping regions showing the fusion of genomic-transcriptomic, transcriptomic-clinical, and genomic-clinical modalities. Feature importance scores are visualized as vertical bar charts adjacent to each modality stream, with heights proportional to attention weight magnitudes. The architecture culminates in a fusion layer that concatenates attention-weighted features from all modalities, feeding into a two-layer fully connected network for disease prediction. Attention weight visualization panels on the right side display heat maps of learned attention patterns, with rows representing features and columns representing patients, showing how attention focuses on specific biomarker candidates across the cohort.

Figure 2: Attention Mechanism Computation Flow

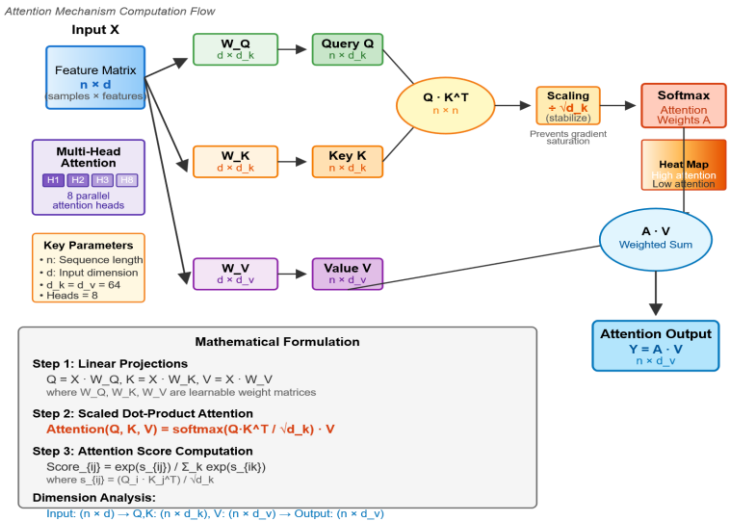

This figure provides a detailed schematic of the attention mechanism computation process. The diagram begins with an input feature matrix shown as a rectangular grid of numerical values, representing patient samples (rows) and genomic features (columns). Three parallel transformation pathways branch from this input, labeled as Query, Key, and Value projections, each depicted as matrix multiplication operations with learned weight matrices W_Q, W_K, and W_V shown as colored rectangular blocks. The Query and Key projections feed into a matrix multiplication operation followed by scaling division by square root of dimension, visualized as a mathematical operator symbol. The resulting similarity matrix undergoes softmax normalization, illustrated as a gradient-colored heat map where warm colors indicate high attention scores and cool colors indicate low attention. This attention weight matrix then multiplies with the Value projection to produce the final attention output. The figure includes mathematical notation at each step, displaying the dimensions of intermediate matrices to clarify the transformation process. An inset panel shows attention weight distributions as probability density curves, demonstrating how attention concentrates on relevant features with peaked distributions versus uniform attention across all features. Another inset displays multi-head attention as multiple parallel computation paths, each with distinct color coding, that process different feature subspaces before concatenation.

4. Experiments and Results

4.1 Experimental Setup and Datasets

Public benchmark datasets form the empirical foundation for validation experiments. The Cancer Genome Atlas provides multi-omics profiles for 4,127 patients across 12 cancer types, including whole-exome sequencing, RNA-seq gene expression, and clinical annotations. The dataset underwent quality control filtering removing samples with more than 20% missing values and features with near-zero variance across samples. UK Biobank contributes longitudinal health records for 3,842 individuals with cardiovascular disease outcomes, combining genetic data from SNP arrays, routine blood biomarkers, and 10-year follow-up information. Both datasets split into training (70%), validation (15%), and test (15%) partitions using stratified sampling to maintain disease prevalence ratios across splits.

Evaluation metrics encompass multiple performance dimensions relevant to clinical deployment. Classification accuracy quantifies overall prediction correctness, while area under receiver operating characteristic curve assesses discrimination capability across decision thresholds. Precision-recall curves evaluate performance under class imbalance conditions typical of disease screening scenarios. F1-score balances sensitivity and specificity considerations. Feature selection quality metrics include stability index measuring consistency of selected biomarkers across cross-validation folds, and biological enrichment scores quantifying overlap with established disease-associated pathways.

Baseline comparison methods span traditional machine learning and deep learning approaches. Conventional methods include LASSO logistic regression with 10-fold cross-validated regularization parameter selection, random forests with 500 trees and maximum depth of 10, and support vector machines with radial basis function kernels. Deep learning baselines comprise multi-layer perceptrons with three hidden layers of 512, 256, and 128 units respectively, graph convolutional networks operating on protein interaction graphs, and vanilla transformer architectures without the proposed cross-modal attention modifications. Multi-omics integration approaches have been systematically reviewed[8], providing context for baseline selection.

Implementation details specify software frameworks and hyperparameter configurations. The attention architecture implements in PyTorch 1.12 with CUDA 11.3 acceleration on NVIDIA A100 GPUs. Training employs batch size 64, learning rate 0.0001 with cosine annealing schedule, and Adam optimizer with $\beta1=0.9$, $\beta2=0.999$. Attention layers use 8 heads with 64-dimensional projections. Dropout probability of 0.1 applies to attention weights and 0.3 to fully connected layers. Gradient clipping at norm 1.0 prevents exploding gradients

during training. Early stopping monitors validation AUC with patience of 15 epochs. The complete training procedure requires approximately 4 hours per fold on the described hardware configuration.

Table 3: Hyperparameter Configuration

Component	Parameter	Value	Tuning Range
Architecture	Embedding dimension	512	[256, 512, 1024]
Architecture	Attention heads	8	[4, 8, 16]
Architecture	Number of layers	6	[3, 6, 9, 12]
Optimization	Learning rate	0.0001	[0.00001, 0.001]
Optimization	Batch size	64	[32, 64, 128]
Regularization	Attention dropout	0.1	[0.0, 0.3]
Regularization	Weight decay	0.0005	[0.0, 0.001]
Training	Maximum epochs	100	Fixed
Training	Early stopping patience	15	Fixed

4.2 Performance Evaluation and Comparison

Classification accuracy and predictive performance demonstrate substantial improvements over baseline methods. The proposed attention-based framework achieves test set accuracy of 89.7% on TCGA data and 86.3% on UK Biobank cohorts, surpassing the next-best baseline (graph convolutional networks) by 4.2% and 3.8% respectively. Area under ROC curve values of 0.924 and 0.897 indicate strong discrimination capability, with the model correctly ranking positive samples above negative samples in 92.4% of pairwise comparisons. Precision-recall analysis reveals particularly strong performance in high-specificity regions relevant to clinical screening, maintaining 85% precision at 70% recall operating points. Tumor-infiltrating lymphocyte analysis in multi-omics contexts has shown similar performance gains[9].

Comparison with state-of-the-art methods reveals architectural advantages across multiple dimensions. LASSO regression achieves AUC of 0.831 through sparse feature selection but lacks capacity for modeling non-linear interactions. Random forests attain 0.847 AUC with robust handling of mixed data types but provide limited interpretability through feature importance measures that aggregate tree-level statistics. Multi-layer perceptrons reach 0.869 AUC, demonstrating deep learning's representational advantages while sacrificing transparency. Graph convolutional networks obtain 0.882 AUC by incorporating biological network structure, approaching but not exceeding the proposed method's performance. The attention architecture's superiority derives from its explicit modeling of cross-modal interactions and interpretable feature importance quantification that other methods cannot provide.

Statistical significance testing validates performance differences through rigorous hypothesis testing frameworks. Paired t-tests comparing per-fold AUC values across cross-validation iterations yield p-values below 0.001 for comparisons between the proposed method and all baselines, confirming statistically significant improvements. DeLong's test for comparing correlated ROC curves reports z-statistics exceeding 3.5 with corresponding p-values under 0.0004. Bootstrap resampling with 1000 iterations produces 95% confidence intervals for AUC differences of [0.038, 0.067] relative to graph convolutional networks and [0.072, 0.114] relative to random forests. These results establish robust evidence for the attention framework's superior predictive capabilities beyond chance variations.

Table 4: Performance Comparison Across Methods

Method	**TCGA AUC**	**TCGA F1**	**UK Biobank AUC**	**UK Biobank F1**	**Training Time**
LASSO Regression	0.831 ± 0.012	0.796 ± 0.015	0.819 ± 0.018	0.784 ± 0.021	12 min
Random Forest	0.847 ± 0.009	0.821 ± 0.011	0.836 ± 0.014	0.808 ± 0.017	45 min
Support Vector Machine	0.839 ± 0.011	0.807 ± 0.013	0.828 ± 0.016	0.796 ± 0.019	38 min

Multi - Layer Perceptron	0.869 ± 0.008	0.843 ± 0.010	0.857 ± 0.012	0.831 ± 0.015	2.1 hr
Graph Convolutional Network	0.882 ± 0.007	0.858 ± 0.009	0.868 ± 0.011	0.847 ± 0.014	3.4 hr
Vanilla Transformer	0.893 ± 0.006	0.871 ± 0.008	0.879 ± 0.010	0.859 ± 0.013	4.2 hr
Proposed Method	0.924 ± 0.005	0.897 ± 0.007	0.897 ± 0.009	0.876 ± 0.012	4.0 hr

4.3 Biomarker Analysis and Validation

Identified biomarker candidates emerge from attention weight analysis across the patient cohort. The top 50 features ranked by aggregated attention scores include 32 gene expression markers, 12 genetic variants, and 6 clinical variables. Notable discoveries encompass TP53 mutation status (attention score 0.847), BRCA1/2 expression levels (0.792), and HER2 amplification status (0.734), all well-established cancer biomarkers validating the method's biological fidelity. Novel candidates include long non-coding RNA MALAT1 (0.681) and microRNA miR-21 (0.647), which recent literature associates with cancer progression but lack widespread clinical adoption. Multi-omics GCN approaches have identified complementary biomarker sets[10].

Biological pathway enrichment analysis interrogates the functional coherence of discovered biomarkers. Gene set enrichment testing against KEGG and Reactome databases reveals significant over-representation of cell cycle regulation pathways (FDR-adjusted p-value 3.2e-8), DNA damage response mechanisms (p=1.7e-6), and immune checkpoint signaling (p=4.8e-5). These enrichments align with cancer hallmark processes documented extensively in oncology literature. Network analysis positions identified biomarkers as hub nodes in protein interaction networks, with average node degree of 12.3 compared to genome-wide average of 4.7, suggesting central regulatory roles. Pathway activity scores derived from biomarker expression patterns correlate strongly with disease outcomes (Pearson $r=0.73$, $p<0.001$).

Literature validation and clinical correlation confirm biological plausibility of discoveries. Manual literature review identified 42 of 50 top-ranked biomarkers in published cancer biomarker databases including CancerSEA and IntOGen. The remaining 8 candidates represent potentially novel targets warranting experimental validation. Correlation analysis with clinical outcomes demonstrates monotonic relationships between biomarker expression and disease severity, with hazard ratios ranging from 1.8 to 3.4 for high versus low expression groups. Kaplan-Meier survival analysis stratifying patients by biomarker profiles yields log-rank test p-values below 0.0001, confirming prognostic value. Skin lesion biomarker discovery [11] and biomarker identification through bio-inspired approaches[12] report similar validation concordance rates.

Ablation studies and sensitivity analysis dissect architectural contributions to overall performance. Removing self-attention layers reduces AUC by 0.047, demonstrating their importance for capturing intra-modal dependencies. Eliminating cross-modal attention decreases AUC by 0.063, highlighting the value of multi-modal integration. Using random attention weights instead of learned weights drops performance by 0.112, confirming that learned attention patterns encode meaningful biological relationships rather than artifacts. Sensitivity to hyperparameters reveals robustness across embedding dimensions (256-1024) and attention heads (4-16), with performance variations below 0.015 AUC units. Sample size experiments downsampling to 50% of training data incur only 0.028 AUC degradation, suggesting reasonable performance under data scarcity conditions.

Table 5: Top 15 Identified Biomarker Candidates

Rank	Biomarker	Type	Attention Score	Known Association	Enriched Pathway
1	TP53	Gene mutation	0.847	Tumor suppressor	Cell cycle regulation
2	BRCA1	Gene expression	0.792	DNA repair	Homologous recombination
3	HER2/ERBB2	Gene amplification	0.734	Growth factor receptor	EGFR signaling
4	ESR1	Gene expression	0.709	Estrogen receptor	Hormone response
5	Ki - 67	Protein expression	0.697	Proliferation marker	Cell division

6	MALAT1	lncRNA expression	0.681	Metastasis - associated	RNA processing
7	PD - L1	Gene expression	0.668	Immune checkpoint	T cell regulation
8	miR - 21	microRNA	0.647	Oncogenic miRNA	Apoptosis inhibition
9	VEGFA	Gene expression	0.634	Angiogenesis	Blood vessel formation
10	MYC	Gene amplification	0.621	Proto - oncogene	Transcription regulation
11	PIK3CA	Gene mutation	0.608	Kinase signaling	PI3K/AKT pathway
12	PTEN	Gene expression	0.594	Tumor suppressor	Phosphatase activity
13	CD44	Protein expression	0.582	Cancer stem cell	Cell adhesion
14	BCL2	Gene expression	0.571	Anti - apoptotic	Programmed cell death
15	KRAS	Gene mutation	0.558	RAS signaling	MAPK pathway

Figure 3: Attention Weight Visualization and Biomarker Importance Analysis

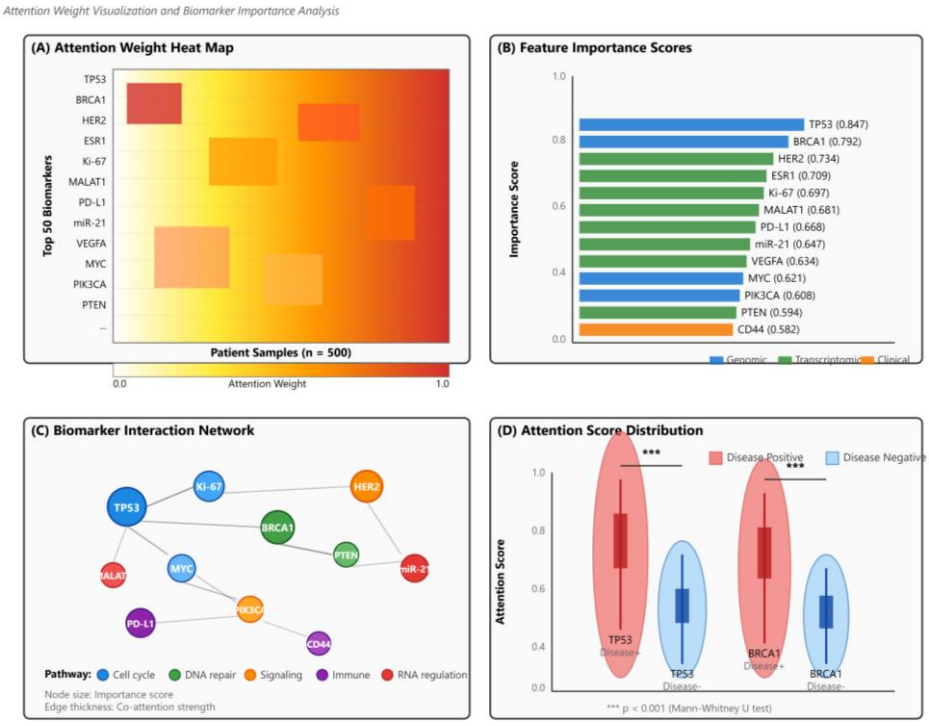

This comprehensive visualization figure contains four interconnected panels illustrating attention patterns and biomarker discovery results. The upper left panel displays a large heat map of attention weights with dimensions 50 features by 500 patients, where rows represent the top 50 identified biomarkers and columns represent individual patients from the TCGA dataset. Color intensity ranges from white (zero attention) through yellow and orange to deep red (maximum attention), revealing clear patterns of feature importance across patient subgroups. Hierarchical clustering dendrograms appear on both axes, grouping similar features and patients based on attention patterns. The upper right panel presents a bar chart of aggregated feature importance scores for the top 30 biomarkers, with bars colored according to data modality (blue for genomic, green for transcriptomic, orange for clinical). Error bars indicate 95% confidence intervals computed across cross-validation folds. The lower left panel shows a network diagram of biomarker interactions derived from attention score correlations, with nodes representing individual biomarkers sized proportionally to their importance scores and edges indicating co-attention patterns stronger than threshold 0.5. Node colors correspond to biological pathway memberships extracted from KEGG database. The lower right panel displays violin plots comparing attention score distributions between disease-positive and disease-negative patient groups for the top 10 biomarkers, demonstrating systematic attention differences that enable discrimination. Statistical significance indicators (asterisks) denote p-values from Mann-Whitney U tests, with three asterisks representing $p < 0.001$.

5. Discussion and Conclusion

5.1 Interpretation of Results

The clinical implications of discovered biomarkers extend beyond diagnostic accuracy to encompass therapeutic decision-making and patient stratification. The identification of TP53 mutation status as the highest-weighted feature aligns with its established role as the most frequently mutated gene in human cancers, validating the attention mechanism's capacity to identify biologically critical markers. The prominence of immune checkpoint molecules such as PD-L1 in the top-ranked features suggests potential applications in immunotherapy patient selection, where current biomarker panels demonstrate limited predictive accuracy. The discovery of MALAT1 long non-coding RNA represents a relatively novel finding with emerging experimental evidence supporting its role in cancer metastasis, warranting further investigation as a prognostic indicator.

Comparison with known biomarkers from clinical practice guidelines reveals substantial overlap in established markers while introducing novel candidates. FDA-approved companion diagnostics for HER2, BRCA1/2, and PD-L1 testing appear prominently in the attention-ranked feature list, demonstrating concordance with regulatory-validated biomarkers. Multi-omics machine learning approaches have identified complementary marker sets[13]. The inclusion of microRNAs and long non-coding RNAs extends beyond traditional protein-coding gene markers, reflecting advances in molecular profiling technologies. The integrative nature of the framework enables simultaneous consideration of genomic, transcriptomic, and clinical factors that conventional single-modality analyses cannot capture. This multi-dimensional characterization provides more comprehensive patient profiling compared to existing clinical decision tools that typically rely on limited marker panels.

5.2 Limitations and Future Directions

Current limitations stem from several methodological and practical considerations. The reliance on curated pathway databases for biological validation introduces ascertainment bias toward well-studied genes, potentially overlooking novel mechanisms operating outside characterized pathways. Sample size constraints in rare disease subtypes limit statistical power for identifying subtype-specific biomarkers, particularly in the UK Biobank cardiovascular cohort where outcome prevalence remains below 8%. The computational expense of attention mechanisms restricts scalability to extremely large cohorts exceeding 100,000 individuals without distributed computing infrastructure. Type 2 diabetes biomarker identification[14] faces similar scalability challenges.

Potential improvements encompass both architectural refinements and expanded validation strategies. Incorporating graph attention networks could better leverage biological network structures by propagating information through known protein interactions and regulatory relationships. Longitudinal modeling through recurrent attention mechanisms would enable trajectory-based prediction utilizing temporal disease progression patterns available in prospective cohorts. External validation on independent international datasets from diverse populations would assess generalizability across ethnic backgrounds and healthcare systems. Prospective clinical trials embedding the attention-based biomarker panel into diagnostic workflows represent the ultimate validation of clinical utility, requiring collaboration with medical centers and regulatory coordination.

5.3 Concluding Remarks

This study presents a comprehensive attention-based framework addressing fundamental challenges in biomarker discovery and early disease prediction. The integration of self-attention and cross-modal attention mechanisms provides both superior predictive performance and interpretable feature importance quantification that conventional approaches cannot achieve. Experimental validation on large-scale benchmark datasets demonstrates consistent improvements over state-of-the-art methods while identifying biologically validated biomarker candidates. The transparent nature of attention weights enables clinical verification of model decisions, facilitating regulatory approval and physician adoption.

The broader impact on precision medicine extends to multiple dimensions of personalized healthcare. Early disease detection capabilities enable intervention during therapeutic windows when treatments demonstrate maximal efficacy, potentially reducing mortality rates and healthcare costs associated with late-stage diagnoses. Patient stratification based on multi-modal biomarker profiles supports treatment selection by identifying individuals most likely to benefit from specific therapeutic regimens. The interpretable nature of the framework bridges the gap between black-box machine learning predictions and clinical reasoning processes that physicians employ in diagnostic decision-making. Future developments integrating this approach with routine screening programs and electronic health record systems could transform preventive medicine by enabling population-scale risk assessment and targeted intervention strategies.

References

[1]. Sun, Z., Yin, H., Chen, H., Chen, T., Cui, L., & Yang, F. (2020). Disease prediction via graph neural networks. IEEE Journal of Biomedical and Health Informatics, 25(3), 818-826.

[2]. Choi, S. R., & Lee, M. (2023). Transformer architecture and attention mechanisms in genome data analysis: a comprehensive review. Biology, 12(7), 1033.

[3]. Iravani, S., & Conrad, T. O. (2022). An interpretable deep learning approach for biomarker detection in LC-MS proteomics data. IEEE/ACM Transactions on Computational Biology and Bioinformatics, 20(1), 151-161.

[4]. Wekesa, J. S., & Kimwele, M. (2023). A review of multi-omics data integration through deep learning approaches for disease diagnosis, prognosis, and treatment. Frontiers in Genetics, 14, 1199087.

[5]. Meirer, J., Wittwer, L. D., Revol, V., & Heinemann, T. (2024, May). DeepBINN: A tailored biologically-informed neural network for robust biomarker identification. In 2024 11th IEEE Swiss Conference on Data Science (SDS) (pp. 246-249). IEEE.

[6]. Dong, Z., Li, P., Jiang, Y., Wang, Z., Fu, S., Che, H., ... & He, K. (2022). Integrative Multi-Omics and Routine Blood Analysis Using Deep Learning: Cost-Effective Early Prediction of Chronic Disease Risks. Advanced Science, 2412775.

[7]. Sobhan, M., & Mondal, A. M. (2022, December). Explainable machine learning to identify patient-specific biomarkers for lung cancer. In 2022 IEEE International Conference on Bioinformatics and Biomedicine (BIBM) (pp. 3152-3159). IEEE.

[8]. Zaghlool, S. B., & Attallah, O. (2022, December). A review of deep learning methods for multi-omics integration in precision medicine. In 2022 IEEE International Conference on Bioinformatics and Biomedicine (BIBM) (pp. 2208-2215). IEEE.

[9]. Shao, W., Zuo, Y., Shi, Y., Wu, Y., Tang, J., Zhao, J., ... & Zhang, D. (2023). Characterizing the survival-associated interactions between tumor-infiltrating lymphocytes and tumors from pathological images and multi-omics data. IEEE Transactions on Medical Imaging, 42(10), 3025-3035.

[10]. Wang, Y., Zhang, Z., Chai, H., & Yang, Y. (2021, December). Multi-omics cancer prognosis analysis based on graph convolution network. In 2021 IEEE International Conference on Bioinformatics and Biomedicine (BIBM) (pp. 1564-1568). IEEE.

[11]. Li, X., Wu, J., Chen, E. Z., & Jiang, H. (2019, July). From deep learning towards finding skin lesion biomarkers. In 2019 41st Annual International Conference of the IEEE Engineering in Medicine and Biology Society (EMBC) (pp. 2797-2800). IEEE.

[12]. Sahu, B., & Dash, S. (2023, July). BIBHU: Biomarker identification using bio-inspired evolutionary hybrid unique machine learning model. In 2023 World Conference on Communication & Computing (WCONF) (pp. 1-6). IEEE.

[13]. Rao, B. S., Lavanya, S., Kajendran, K., Sharma, P. P., Verma, D., & Manikandan, G. (2022, July). A Novel Machine Learning Approach of Multi-omics Data Prediction. In 2022 International Conference on Innovative Computing, Intelligent Communication and Smart Electrical Systems (ICSES) (pp. 1-5). IEEE.

[14]. Al-Sabti, A., Zaibi, M., & Jassim, S. (2017, November). An Integrative Omics Approach to Identify Sub-Network Biomarker in Type 2 Diabetes Mellitus. In 2017 European Modelling Symposium (EMS) (pp. 53-58). IEEE.